Philippine Journal of Science
149 (4): 1083-1094, December 2020
ISSN 0031 - 7683
Date Received: 22 Jun 2020

Removal of Coomassie Brilliant Blue R-250 Using Iron Oxide-Graphene Oxide Composite *via* Fenton-like Reaction

Al Jerome A. Magsino*, Christine Joy T. Carlos, Mary Ann O. Torio, Teofila DC. Villar, Myrna S. Rodriguez, and Mae Joanne B. Aguila*

Institute of Chemistry, College of Arts and Sciences
University of the Philippines Los Baños
College Laguna 4031 Philippines

The presence of organic dyes in the environment greatly affects the photosynthetic capabilities of underwater organisms as these compounds block sunlight and reduce the amount of available oxygen. Moreover, the structural diversity of dyes makes them highly resistant to light, heat, and oxidizing agents; thus, new approaches for dye remediation are continuously being developed. The use of iron oxide-graphene oxide composite (IOGOC) with persulfate oxidant via a Fenton-like reaction for the removal of Coomassie Brilliant Blue (CBB) R-250 in aqueous solutions was investigated. The IOGOC adsorbent was synthesized and then characterized using FTIR (Fourier-transform infrared spectrophotometry), SEM (scanning electron microscope), and XRD (X-ray powder diffraction). Adsorption isotherm and kinetic studies revealed that the adsorption of the dye on IOGOC was best described by Langmuir isotherm with a maximum adsorption capacity of 14.31 ± 0.65 mg CBB R-250/ g IOGOC and followed the pseudo-second-order kinetic model. Batch adsorption studies were done to determine the effect of dye concentration, adsorbent loading, oxidant concentration, and pH on dye removal. Results showed that the parameters for the dye degradation that afforded a significantly higher degree of dye removal were 10 mg/L adsorbate amount at pH 3.0 with 7 mg adsorbent loading and 3 mM persulfate solution for 270 min contact time. End product analyses indicate that the treated water sample contains 1.84 ± 0.30 mg dissolved iron/ L solution, which is within the limits based on Department of Environment and Natural Resources' (DENR) Water Quality Guidelines and General Effluent Standards of 2016 and a 73 ± 19% chemical oxygen demand (COD) removal. Recyclability studies show that the synthesized composite can be used for four times without a significant decrease in the dye removal efficiency.

Keywords: Coomassie Brilliant Blue R-250, dye removal, Fenton-like reaction, graphene oxide, iron oxide

INTRODUCTION

Water pollution has been one of the most challenging problems faced by humanity today. According to the United Nations World Water Development Report of 2017, the degree of pollution affects 245,000 m^2 of the Earth's ecosystem. In an agricultural-based country like the Philippines, water pollution is also rampant as agricultural activities – coupled with increased population and industrialization – continue to reduce the water quality. According to the Water Environment Partnership in Asia, the damage dealt by all the activities contributing to water pollution in the Philippines amounts to $1.3 B annually (Andrews 2018).

*Corresponding Authors: aamagsino@up.edu.ph
mbaguila@up.edu.ph

There are different factors contributing to poor water quality. Agrochemical wastes generated from excess pesticide and fertilizer usage can introduce dangerous organic compounds in different bodies of water through leaching. Domestic sewage in water may contain hazardous pathogens that can pose serious health problems in humans. Waste products from several industrial manufacturing plants may contain heavy metals and other organic compounds (Alrumman 2016). Combined effects of all these factors highly disrupt the marine ecosystems and, by extension, human ecology.

One of the major industrial sectors that produce large amounts of wastewater is the textile industry. Effluents of the textile industry typically contain organic dyes, organochlorines, and some heavy metals. Although dye contamination is less serious of a threat compared to heavy metals, dye solutions still pose some risks due to its intense color in solutions, even at low concentrations. This property of dyes in water affects the photosynthetic capabilities of marine organisms as these compounds block sunlight and reduce the amount of available oxygen. Moreover, organic compounds that make up the dyes are structurally diverse and are highly resistant to light, heat, and oxidizing agents – making it difficult to create a universal method for dye degradation. Several studies focus on the development of methods to remove organic dyes from aqueous solutions and apply these methods to actual wastewaters contaminated by dyes (Clarke and Anliker 1980; Robinson *et al.* 2001; Sun and Yang 2003).

CBB R-250 is a dye utilized in the textile industry and, recently, in biochemistry and other related research laboratories as a protein staining agent. There is currently a buildup of CBB R-250 in laboratories in the university due to regular protein analyses done both in teaching and research laboratories.

The use of graphene oxide (GO) based materials for dye removal has been extensively utilized as adsorbents recently due to its large surface area and added functionalization, which can create more interactions with the target contaminant. Iron-based compounds are also being explored as adsorbents due to their magnetic capabilities that are useful in the adsorbent recovery process. Other approaches to contaminant removal involve degradation of the target compound. Fenton reactions make use of hydroxyl radicals generated from hydrogen peroxide, and these reactions are known to be fast compared to other pollutant removal methods but create additional waste in the form of the iron ions from the metal catalyst (Nidheesh 2013).

This study aims to use an IOGOC that will adsorb and degrade CBB R-250 *via* a Fenton-like reaction. The process of the dye removal in this method will make use of little amounts of the adsorbent and the oxidant for degradation so that little to zero added toxicity is introduced. The adsorbent is also designed to be magnetic in nature in order to ease its separation process from wastewater by simply applying an external magnetic field on the mixture, thus providing a more environmental-friendly alternative for CBB R-250 removal in wastewater. This can help reduce the increasing amount of CBB R-250 waste generated in research and teaching laboratories in the university.

MATERIALS AND METHODS

GO and IOGOC Synthesis

GO was synthesized using the modified Tour method (Marcano 2010). A 9:1 H_2SO_4: H_3PO_4 solution was added to a mixture of 1.0 g of graphite and 6.0 g of potassium permanganate and stirred for 12 h at 50 °C. The resulting mixture was cooled to room temperature and poured into around 400 g of ice. It was then treated with 30% hydrogen peroxide until the disappearance of the purple color, and the resulting yellow mixture was allowed to stand for 24 h and decanted to obtain yellow-brown solids. The solids were washed several times with 10% HCl then distilled water until pH 7.0. The mixture was then sonicated for 2 h followed by centrifugation at 500 rpm for 90 min. The supernatant containing the GO was then centrifuged at 9000 rpm for 15 min. The solids recovered were washed with distilled water and dried at 45 °C for 24 h. The process produced dark brown powder with a 69.17% conversion.

The IOGOC was synthesized using the co-precipitation method (Zhang 2015). A GO solution was slowly added to an aqueous solution of $FeCl_3 \cdot 6H_2O$ and $FeSO_4 \cdot 2H_2O$. Ammonia solution was added quickly to the resulting mixture until pH 10 and heated to 85 °C with rapid stirring for 45 min. The mixture was then cooled to room temperature and separated magnetically. The formed solids were washed with deionized water and ethanol followed by drying at 60 °C for 48 h. The reaction afforded black solids with 41.08% conversion.

The synthesized products were characterized using Thermo Scientific MultiSkan™ GO microplate spectrophotometer, Shimadzu IR Prestige-21 FTIR unit equipped with single reflection diamond ATR (attenuated total reflection) accessory, Shimadzu LabX XRD-6100 unit, and Quanta 250 FEG SEM.

Determination of Adsorption Isotherm and Adsorption Kinetics

The adsorption isotherm model for the system was determined by using different concentrations of CBB R-250. A mixture containing 5.0 mg of IOGOC and 25 mL

of CBB R-250 solution was incubated with stirring (200 rpm) at 25°C until it reached the adsorption-desorption equilibrium. The remaining amount of CBB R-250 in the supernatant was monitored over the course of the adsorption process using UV-Vis (ultraviolet-visible spectroscopy) at 550 nm. The amount of dye removed was calculated using the formula:

$$\%\ dye\ removed = \frac{C_o - C_t}{C_o}\ x\ 100 \quad (1)$$

where C_o is the initial dye concentration and C_t is the concentration at time = t.

The adsorption capacity (Q_e) was also calculated using the formula:

$$adsorption\ capacity\ \left({}^{mg\ dye}/_{g\ adsorbent}\right) = \frac{(C_o - C_e) * V_{soln}}{m_{ads}} \quad (2)$$

where C_o is the initial dye concentration, C_e is the equilibrium dye concentration, V_{soln} is the volume of the solution used, and m_{ads} is the adsorbent loading.

The equilibrium adsorption data were fitted to Langmuir, Freundlich, Temkin, and the Dubinin-Radushkevich isotherm; adsorption kinetics data were fitted to pseudo-first-order, pseudo-second-order, and Elovich model.

Evaluation of Different Parameters of the Adsorption-Degradation Process

All adsorption-degradation experiments were done in batch with constant stirring (200 rpm) at 25 °C using Labnet Orbit™ 1900 high capacity lab shaker. For the effect of initial dye concentration, 5.0 mg of IOGOC was added to 25 mL of acidic dye solutions (pH = 3.0) at different concentrations (10, 20, 30, 40, 50 mg/L) and was stirred for 90 min. The calculated mass of potassium persulfate was then added (1 mM) to initiate the Fenton-like reaction and the resulting mixture was stirred for 180 min.

For the effect of adsorbent loading, different amounts of the adsorbents (5, 7, 10 mg) were applied to 25 mL of 10 mg/L dye solution at pH 3.0 and stirred for 90 min. The concentration of persulfate in the resulting solution was kept at 1 mM and then incubated for 180 min.

The effect of persulfate concentration on the degradation efficiency of the process was done by using a constant amount of dye at 10 mg/L at pH 3.0 with 5 mg of IOGOC adsorbent. The mixture was allowed to equilibrate for 90 min. Different amounts of potassium persulfate were then added (1 mM, 3 mM, 5 mM). The mixture was then stirred for 180 min.

Different working pH values (3, 7, 9) for the initial dye solution were used following the same protocol with 10 mg/L dye concentration, 5 mg of IOGOC, and 90 min of stirring. A calculated amount of persulfate was added to afford a final concentration of 1 mM, followed by stirring for 180 min.

After the designated contact time, IOGOC was separated from the mixture by applying a magnet, and the remaining dye in the solution was determined at 550 nm.

Comparison Studies

The degree of dye removal of the synthesized adsorbent *via* a Fenton-like reaction was compared with other substances [GO only, iron oxide (Fe_3O_4) only, persulfate only, and IOGOC only]. Five milligrams (5 mg) of the substance was added to 25 mL of 30 mg/L CBB R-250 solution, and the resulting mixture was allowed to reach equilibrium for 90 min at 25°C with continuous shaking at 200 rpm. The calculated amount of potassium persulfate (1 mM) was then added to applicable treatments and then incubated for 180 min. The remaining dye in the supernatant was determined using UV-Vis at 550 nm.

Adsorbent Regeneration Study

The recyclability of the adsorbent was evaluated by repeatedly using the IOGOC adsorbent. The used IOGOC was first washed with an acid solution (HCl, pH = 3.0) followed by ethanol. The solids were then washed repeatedly with distilled water until neutral. The adsorbent was then dried at 50 °C prior to use.

Iron Leaching Analysis

Prior to analysis, the degradation process was done by adding 10 mg of IOGOC to a 20 mg/L CBB R-250 solution at pH 3.0. Appropriate persulfate (5 mM) was then added to the mixture, and the resulting mixture was stirred for 240 min at 25 °C. For dissolved iron analysis, additional runs with 5.0 mg $FeSO_4$ and 5.0 mg $FeCl_3$ as iron sources – instead of IOGOC – were done to compare the degradation performance of IOGOC with other water-soluble iron sources.

The leached iron in the solution from the composite was determined *via* the phenanthroline method (Eaton *et al.* 1998). A 2.0 mL concentrated HCl and 1.0 mL of hydroxylamine solution (0.1 g/mL) were added to a 25-mL supernatant obtained after the degradation process. The volume of the resulting solution was reduced to around 15 mL by boiling the solution. The solution was then cooled to room temperature and transferred to a volumetric flask. An ammonium acetate buffer solution and 4.0 mL of phenanthroline solution (1 mg/mL) were then added to the cooled mixture and diluted to mark. Color development was done by standing the mixture for 10–15 min. The absorbance of the solution was obtained using UV-Vis

spectrophotometry at 510 nm. The iron concentration in the solution was calculated by regression analysis using a standard calibration curve, with ferrous ammonium sulfate as the standard.

Organic Product Analysis

The COD after treatment was done using the standard dichromate method for wastewater analysis (Eaton *et al.* 1998). A 2.5-mL water sample was placed into a 25 x 100 mm tube, then 1.5 mL of the dichromate digestion solution, and 3.5 mL of the catalyst solution (Ag_2SO_4 in sulfuric acid) were added to the sample. The mixture was heated at 150 °C for 2 h. The hot mixture was allowed to cool slowly to room temperature. The resulting solution was titrated using a standardized $Fe(NH_4)_2(SO_4)_2$ (standardized against potassium dichromate), with ferroin as the indicator. A color change from yellow/green to red-orange was treated as the endpoint. Blank COD determinations were done using distilled water.

RESULTS AND DISCUSSION

Characterization of GO and IOGOC

Aqueous GO was analyzed using UV-Vis in order to verify the identity of the dispersion (Figure 1A). From the absorbance spectrum, it can be seen that there is an absorbance peak around 230 nm, which corresponds to a π-π* transition in the aromatic portions (C=C) of GO. This plasmon peak, however, is also present in graphite. The differentiating feature in the absorbance spectrum is the weak shouldering around 310 nm. This signal is due to the n-π* transition in the epoxide (C-O-C) and peroxide (C-O-O-C) like linkages that could be present in GO (Saxena *et al*. 2011; Mura *et al*. 2018). The IOGOC was not subjected to UV-Vis since it does not disperse readily in water.

FTIR analysis of GO and IOGOC confirmed the presence of functional groups on the synthesized materials (Figures 1B and 2A). Signal at around 3100–3200 cm^{-1} indicates the O–H bond stretches in both materials. This can be attributed to either the hydroxyl groups covalently attached to GO or residual water molecules adsorbed on the surface of the GO and IOGOC. The signal at 1047 cm^{-1} implies C–O bond stretches, which confirms the presence of epoxy groups on the synthesized GO. The 1739 cm^{-1} peak corresponds to C=O bond stretching of the –COOH groups in GO. This shifts to 1593 cm^{-1} for IOGOC since the carboxylic acid moiety is deprotonated during the synthesis of IOGOC (Yang *et al.* 2009; Mura *et al*. 2018). The observed bands at the 400–600 cm^{-1} region correspond to Fe-O lattice vibrations. The characteristic IR bands of magnetite are at 578.64 cm^{-1}, which indicates Fe-O stretching mode of the tetrahedral and octahedral sites and at 408.91 cm^{-1}, which indicates Fe-O stretching mode of the octahedral sites given that the Fe^{3+} ion displacements at the tetrahedral sites are negligible (Namduri and Nasrazadani 2008; Li *et al*. 2012; Pérez-Guzmán *et al*. 2020). According to Barik and co-workers (2014), hematite has a characteristic FTIR band at 474 cm^{-1}, which pertains to a Fe-O bending mode. The presence of a band at 451.34 cm^{-1} and the other characteristic bands of magnetite indicate that the synthesized IOGOC could contain both magnetite and hematite.

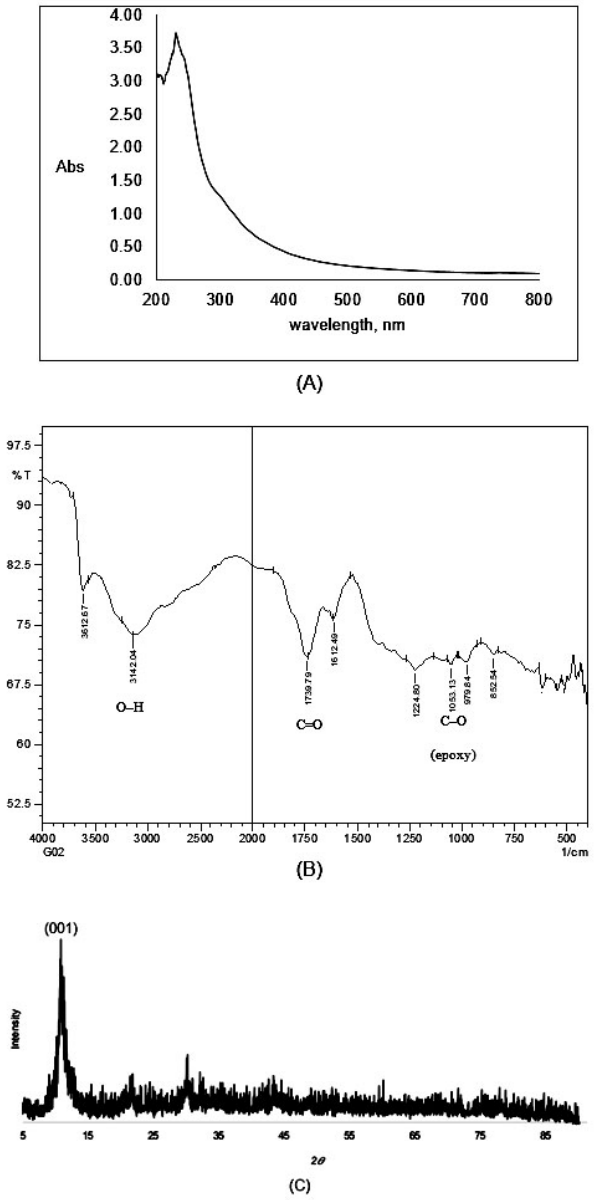

Figure 1. Characterization of GO: (A) UV-Vis, (B) ATR-IR, and (C) XRD.

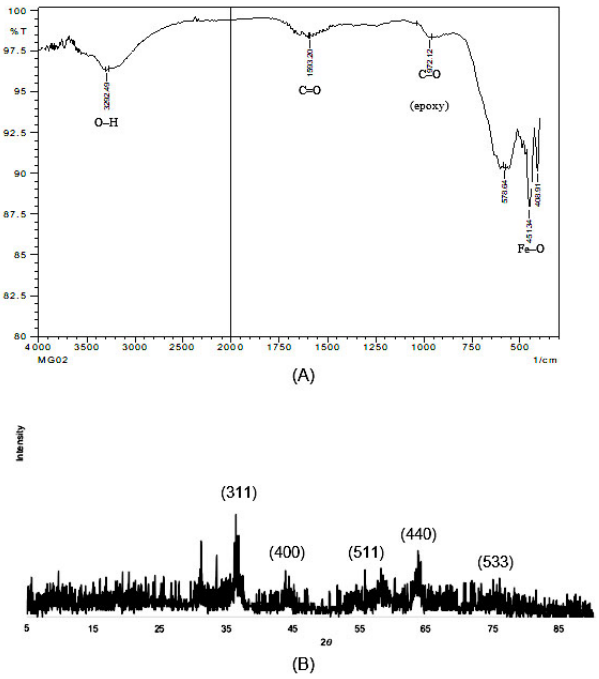

Figure 2. Characterization of IOGOC: (A) ATR-IR and (B) XRD.

XRD analysis was done for both GO and IOGOC samples to further confirm the identity of synthesized materials (Figures 1C and 2B). Based on the XRD pattern of synthesized GO, it can be seen that there is a diffraction peak at $2\theta = 10.81^{o}$ with a *d*-spacing of 8.18189 Å, which is a characteristic diffraction peak of the (001) crystal plane of GO (Johra *et al.* 2014). For the synthesized IOGOC, diffraction peaks at the following 2θ values were observed: 36.45°, 44.18°, 57.02°, 63.67°, and 75.52°, which could possibly correspond to the (311, 400, 511, 440, and 533) crystalline planes of magnetite (Ouyang *et al.* 2015; Pérez-Guzmán *et al*. 2020). The observed interplanar spacing *d*-values of the respective crystalline planes of IOGOC (2.46970, 2.04837, 1.61377, 1.46046, and 1.25786 Å) are also comparable to the reported values of Gupta and co-workers (2016) on synthesized magnetite.

Scanning electron microscopy was also used to study the morphology of the synthesized GO, Fe_3O_4, and IOGOC (Figure 3). It can be seen that the synthesized GO has around 1.5–2.0 μm thickness and the Fe_3O_4 particles are at the nanoscale. The micrograph in Figure 3C shows that the synthesized product contains both GO and Fe_3O_4, as indicated by the combination of the structural features of the individual components seen in the other micrographs (Figures 3A and 3B).

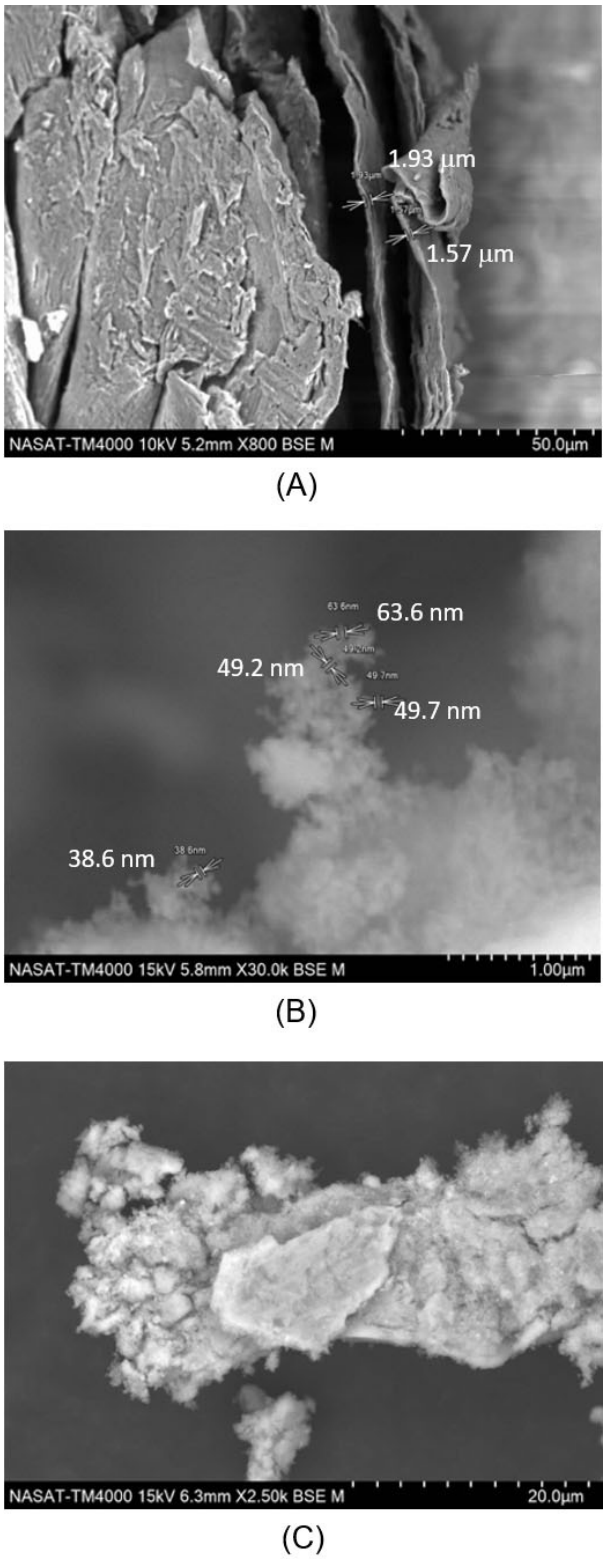

Figure 3. SEM of synthesized materials: (A) GO, (B) Fe_3O_4, and (C) IOGOC.

Adsorption Isotherm and Kinetic Modelling

Adsorption data were fitted to different isotherm models (Table 1) and the adsorption of CBB R-250 on IOGOC

Table 1. Parameter estimates of various adsorption isotherm models.

Isotherm model	Parameter	Estimated value
Langmuir ($r^2 = 0.991$)	Q_m (mg/g)	16.46
	K_L (L/g)	0.143
Freundlich ($r^2 = 0.967$)	K_f (mg/g)	4.776
	n	3.353
Temkin ($r^2 = 0.977$)	A_T (L/g)	1.837
	B_T	750.157
	B (J/mol)	3.304
Dubinin-Radushkevich ($r^2 = 0.875$)	Q_s (mg/g)	33.052
	K_{ad} (mol^2/J^2)	1.565×10^{-5}
	E (kJ/mol)	0.179

follows the Langmuir isotherm, based on the obtained linearity coefficient. This implies that CBB forms a monolayer on the surface of the IOGOC composite and no additional layers of the dye are adsorbed (Foo and Hameed 2010).

A key feature of the Langmuir isotherm model is the separation factor R_L, where K_L is the Langmuir constant and C_0 is the initial concentration of the adsorbate:

$$R_L = \frac{1}{1 + K_L C_0} \quad (3)$$

A separation factor value greater than one indicates an unfavorable adsorption process while a $0 < R_L < 1$ suggests favorable adsorption. With a calculated R_L value of 0.123–0.412 over the working concentration range, the adsorption of CBB R-250 on IOGOC is considered a favorable process.

The experimental maximum CBB R-250 adsorption capacity on IOGOC is 14.31 ± 0.65 mg CBB/g IOGOC. The obtained maximum adsorption capacity is quite close to the predicted Q_m of 16.46 mg CBB/g IOGOC using the Langmuir isotherm model. The adsorption capacity of CBB on IOGOC is compared to the adsorption capacity of CBB on other adsorbents, as well as the adsorption of other organic dyes with GO-related adsorbents (Table 2). The obtained adsorption capacity on IOGOC is relatively low compared to those previously reported. This can be due to the differences in the nature of adsorbent, as well as the differences in adsorption parameters done in the study. Ramesha and co-workers (2011) proposed that anionic dyes such as CBB R-250 do not effectively adsorb on GO surfaces because of the presence of the sulfonate groups. The negative charge on these moieties causes repulsion with the negative portions of GO, as opposed to the use of a cationic adsorbent [*e.g.* polyaniline (PANI)], which allowed more CBB to be adsorbed on the synthesized adsorbent. Moreover, all adsorption processes involving the cationic dye (*e.g.* methylene blue) had higher adsorption capacities while anionic dyes (*e.g.* Acid Orange 8) had lower adsorption capacities. The driving forces for the relatively favorable adsorption of CBB R-250

Table 2. Obtained adsorption capacities of CBB R-250 on some adsorbents.

Adsorbent	Experimental conditions	Adsorption capacity (mg adsorbate/g adsorbent)	Reference
Natural agalmatolite	[CBB] = 25 mg/L, m_{ads} = 100 mg, pH = 2	11.29	Sales *et al.* (2013)
Wheat bran	[CBB] = 10 mg/L, [ads] = 2 g/L, pH 2	6.41	Ata *et al.* (2012)
PANI emeraldine salt	[CBB] = 50-500 mg/L, m_{ads} = 100 mg, 2h	129	Mahanta (2008)
PNCoFe-80	[CBB] = 100 mg/L, m_{ads} = 100 mg, 240 min	45.39	Khan *et al.* (2015)
GO/ chitosan composite (Acid Red)	[dye] = 1500 mg/L, m_{ads} = 100mg, pH = 3.0, 30°C	255	Li *et al.* (2015)
GO (Acid Orange 8/ Direct Red 23)	[dye] = 10–50 mg/L, m_{ads} = 40 mg, 20°C	29.0/15.3	Konicki *et al.* (2017)
Layered GO (Methylene Blue/ Malachite Green)	[dye] = 20 mg/L, m_{ads} = 100 mg, pH = 3	220/180	Bradder *et al.* (2011)
Fe_3O_4/ SiO_2 core/ shell nanoparticles on GO (Methylene Blue)	[dye] = 25 mg/L, m_{ads} = 10 mg, 25 °C	97.0	Yao *et al.* (2012)
IOGOC	[CBB] = 50 mg/L, m_{ads} = 5 mg, pH = 3	14.31	This study

on the synthesized composite are the hydrogen bonding modes that exist among carboxylic portions of GO and polar moieties (*i.e.* sulfonate) of CBB R-250, as well as some electrostatic interaction between CBB and iron-oxygen portions of the adsorbent. According to Herrera and co-workers (2001), the surface structure of hematite – Fe_2O_3, where all the iron ions are in the +3 oxidation state – can undergo proton exchange at different pH values. Considering that the synthesized material has the same functionalities as hematite and behaves the same at different pH conditions, at pH = 3.0, the existing form of the iron component at the surface of the adsorbent may be $[Fe(OH_2)]^+$. Protonation of the surface oxygen in hematite can give rise to favorable electrostatic interactions with CBB R-250, which is anionic in nature.

Kinetic studies on CBB R-250 adsorption on IOGOC showed that the adsorption process follows a pseudo-second-order kinetic model (Table 3). Moreover, the experimental adsorption capacity for process agrees better with the predicted adsorption capacity using the pseudo-second-order model (14.1 mg CBB/g IOGOC), which is comparable to studies that involve adsorption of organic dyes on GO-based composites and CBB R-250 on synthesized composites (Ata 2012; Yao *et al.* 2012; Sales *et al.* 2013; Khan *et al.* 2015; Li *et al.* 2015; Konicki *et al.* 2017). The pseudo-second-order adsorption kinetics indicates that the uptake rate is second order with respect to the adsorption sites (Tan and Hameed 2017).

Evaluation of Degradation Parameters

The degradation of CBB R-250 was tested using the synthesized IOGOC and persulfate as the oxidant *via* a Fenton-like reaction. The Fenton reaction in this study involves the activation of the persulfate to produce sulfate radicals in the presence of Fe^{2+} present in the magnetite structure of the synthesized composite. The GO

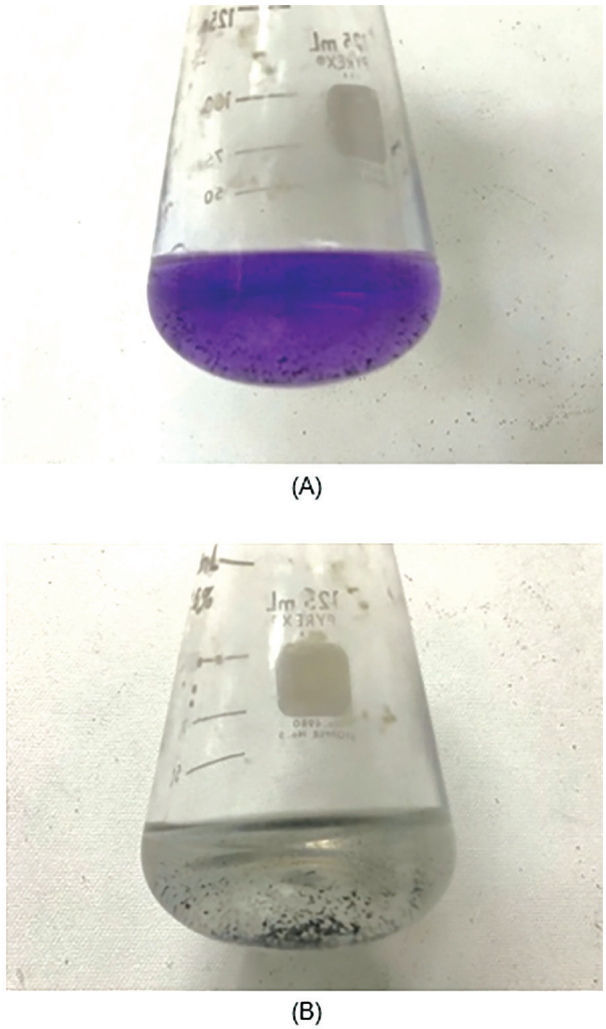

Figure 4. Degradation of CBB R-250 using IOGOC as iron source and persulfate as oxidant (A) before and (B) after treatment. Conditions: initial [CBB] = 20 mg/L, m_{ads} = 10 mg, [PS] = 5 mM, pH = 3.0, T = 25 °C, adsorption time = 90 min, degradation time = 240 min, shaking velocity = 200 rpm.

Table 3. Kinetic model parameters for CBB R-250 adsorption on IOGOC.

Kinetic model	Linear form of equation	Rate constant (k)	R^2	Calculated q_e (mg adsorbate/ g adsorbent)
Pseudo-first order	$\ln(q_e - q_t) = lnq_e - k_1 t$	0.0283 min^{-}	0.8813	10.71
Pseudo-second order	$\frac{t}{q_t} = \frac{1}{k_s q_e^2} + \left(\frac{1}{q_e}\right) t$	0.6544 g/mg min	0.9882	14.10
Elovich model	$q_t = \frac{1}{\beta}\ln(\alpha\beta) + \frac{1}{\beta} lnt$	–	0.9064	–
Experimental				14.67

Conditions: initial [CBB R-250] = 20 mg/L, m_{ads} = 5 mg, pH = 3.0, T = 25 °C, contact time = 90 min, stirring condition = 200 rpm

component was added as support and to reduce the degree of agglomeration of magnetite to improve the degradation efficiency of the reaction. The physical changes associated with the overall removal of CBB using IOGOC is shown in Figure 4. CBB R-250 under acidic conditions initially has a bluish to a purplish color. After treatment with IOGOC and persulfate oxidant, there was decolorization of the resulting solution as the dye was removed by either adsorption on the surface of IOGOC or degradation of the dye structure under the influence of the persulfate oxidant, or a combination of both these effects.

Successful degradation of CBB R-250 under the given conditions is confirmed due to a higher degree of dye removal compared to the sole adsorption process. Several parameters were evaluated in order to gauge a possible working condition for the degradation of CBB R-250 using IOGOC. All calculated percentage removal values are expressed as mean ± standard deviation (SD) (n = 3) and compared using Tukey's honestly significant difference test ($p < 0.05$).

Effect of pH

A significantly higher amount of dye was removed at pH 3.0 (58.02 ± 4.31%) than pH 7.0 (31.33 ± 3.30%). The Fenton and Fenton-like reactions work well in acidic conditions since hydronium ions are required to catalyze the formation of the sulfate radicals. Also, the decrease in the amount of dye degraded for neutral dye solution can be attributed to the decomposition of the persulfate activator (Li *et al.* 2018) and formation of iron hydroxides, which inhibit the release of iron ions in solution for catalysis, thus decreasing the degree of activation of the oxidant (Govindan 2015). At pH 9.0, 52.22 ± 1.61% of the initial dye amount was removed. This is significantly different from the neutral run but not significantly different from the acidic run. This high value despite the inactivation of iron due to hydroxide formation is due to partial activation of the persulfate oxidant under alkaline conditions (Furman 2010). The reaction of aqueous persulfate ion and hydroxide forms hydroperoxide ion (Equation 4) and its reaction with another unit of persulfate generates the sulfate radical as well as peroxide radical (Equation 5). All runs were carried out using pH 3.0 since it is the recommended pH for the Fenton reaction, and the CBB wastes generated in biochemistry laboratories are already acidic, thus eliminating the need for pH adjustment prior to treatment.

$$S_2O_8^{2-} + 2H_2O \xrightarrow{^{-}OH} HO_2^- + 2SO_4^{2-} + 3H^+ \quad (4)$$

$$S_2O_8^{2-} + HO_2^- \rightarrow SO_4^{\cdot-} + SO_4^{2-} + H^+ + O_2^{\cdot-} \quad (5)$$

Effect of Dye Concentration

The data indicate that the 10 mg/L initial dye concentration resulted in the highest amount of dye removed (58.02 ± 4.31%), which is significantly different from all of the other concentration values. At higher dye concentrations, more dye molecules are available. And with a limited amount of composite, there could be a decrease in the possible sites for adsorption, especially since it only allows the formation of a monolayer adsorbate according to the Langmuir isotherm. Another reason is the limited amount of persulfate added in the dye solutions. At 1mM persulfate concentration, the oxidant could be exhausted easily and the sulfate radical generated is simply not enough to carry out degradation of all dye molecules. The high dye removal efficiency was observed in the study of Rasoulifard and co-workers (2018) with their work on C.I. Direct Blue 129 degradation, and in that of Chen *et al.* (2012) for UV-assisted activation of persulfate on the degradation of rhodamine B at low initial dye concentrations.

Effect of Adsorbent Loading

Results show that a higher dose of adsorbent leads to a higher amount of dye removed from the solution even at a constant amount of persulfate, although there is no significant difference between 7-mg (77.89 ± 1.30%) and 10-mg adsorbent loading (80.93 ± 0.65%). A 20% increase in the dye removal efficiency for 7-mg loading, as compared to 5-mg loading (58.02 ± 4.31%), can be accounted to the higher number of possible adsorption sites for the dye as well as higher amounts of iron that will promote the radical formation of the persulfate oxidant.

Effect of Persulfate Concentration

An increase in the persulfate concentration resulted in a significant increase in the dye removal efficiency under the set conditions for 1 mM (58.02 ± 4.31%) and 3 mM (74.56 ± 1.96%) persulfate solution. There is also an increase in dye removal from 3 mM to 5 mM (81.92 1.92%) but the difference is not significant in accordance with Tukey's test. A low concentration of persulfate indicates that there is a low amount of the sulfate radicals that can be generated *via* iron activation. The increase in persulfate concentration favored the production of more radicals and also decreased the pH of the resulting solution, which favored the release of iron ions in solution to catalyze CBB degradation (Weng and Tao 2015).

Comparison Studies

The efficiency of the synthesized composite in removing CBB R-250 was compared to its individual components. The highest dye removal percentage was observed for IOGOC coupled with persulfate oxidant at 46.51 ± 3.09%,

while there is 11.53 ± 1.92% and 12.67 ± 1.95% removal for the adsorbent only and the oxidant only, respectively. A lower value is expected for IOGOC only since the mode of dye removal in the absence of persulfate oxidant is *via* adsorption on the surface of IOGOC. The run with the activator but without the iron source afforded the same degree of dye removal. This can be due to other factors that initiated the formation of the persulfate radical such as the presence of hydroxide ions, heat, and light.

IOGOC (46.51 ± 3.09%) was able to remove a significantly higher amount of dye compared to GO (22.07 ± 4.23%) and Fe_3O_4 (32.67 ± 2.70%) under the same reaction conditions. The combination of the two components offered an increase in the overall removal of CBB R-250 in an aqueous medium. The obtained percentage removal with GO can be primarily due to the adsorption of CBB R-250 on the material. Fe_3O_4, in the presence of the oxidant, is expected to remove more dye molecules from the solution since persulfate is activated and there is also probable adsorption of some dye molecules on the surface of magnetite.

Iron Leaching Analysis

The dissolved iron was quantified using the phenanthroline method in order to gauge the extent of iron leaching from the synthesized composite. Prior to the analysis, the changes in the absorbance curves of solutions after treatment using different iron sources were obtained (Figure 5). It can be seen from Figure 5A that there is an absorbance peak around 550 nm, which corresponds to the absorption of the chromophore of CBB R-250. After treatment, there is a decrease in the absorbance of the solution at the same wavelength and an increase in the absorbance around 450 nm, which can be attributed to the presence of ferric ions in solution.

The IOGOC was able to remove 79.48 ± 7.01% of CBB R-250 while the use of $FeCl_3$ and $FeSO_4$ removed 75.72 ± 2.88% and 69.02 ± 3.78%, respectively. There is also a low amount of iron present in the solution for IOGOC (1.84 ± 0.30 mg Fe/L) as compared to the soluble iron sources – 40.51 ± 3.73 ppm for $FeSO_4$ and 53.10 ± 1.66 ppm for $FeCl_3$. This indicates that the use of IOGOC decreases the dissolved iron present in solution with comparable degradation efficiency with soluble iron sources. Moreover, the amount of iron that leaches out of the source is within the limit set by the DENR AO 2016-08: Water Quality Guidelines and General Effluent Standards of 5–35 mg Fe/L for Class A to Class D water.

Organic Product Analysis

The COD is a measure of the oxygen equivalent of the organic matter in a water sample that is susceptible to oxidation by strong oxidizing agents such as potassium permanganate and potassium dichromate. It is expected

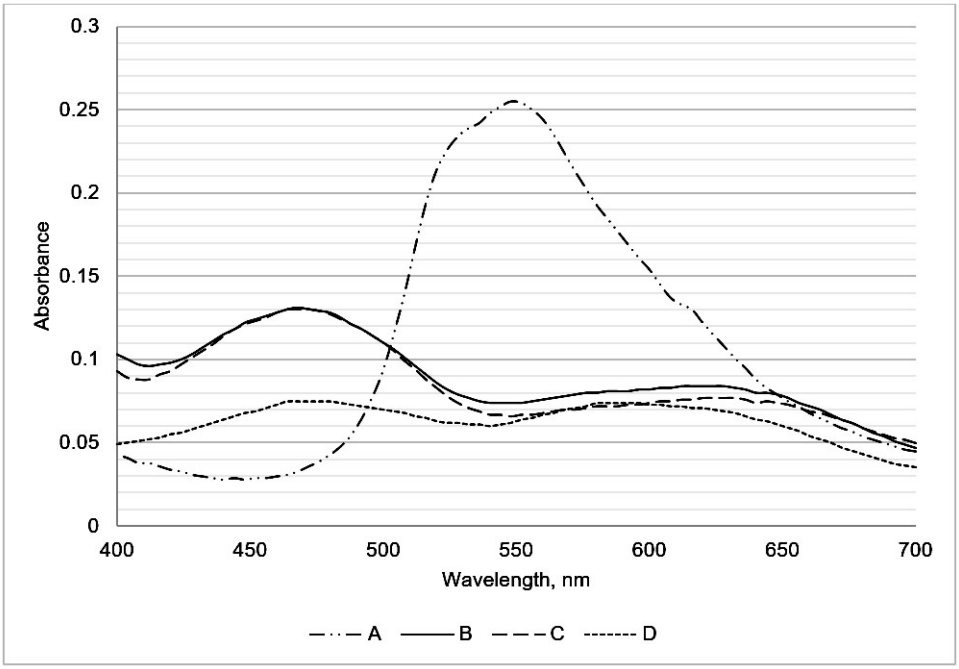

Figure 5. Absorbance curve of (A) CBB R-250 solution before treatment, (B) CBB R-250 solution after treatment using $FeSO_4$ as iron source (5 mg), (C) CBB R-250 solution after treatment using $FeCl_3$ as iron source (5 mg), and (D) CBB R-250 solution after treatment using IOGOC as iron source (10 mg).

that after the degradation process, there should be a decrease in the amount of organic matter and, subsequently, in the COD of the resulting aqueous solution. There was a 73 ± 19% COD removal upon treatment with the synthesized catalyst, which is comparable with the work of Baburaj *et al.* (2012) and Paz *et al.* (2017) on CBB removal. However, obtained COD of the supernatants after treatment is still higher than the recommended COD levels for different water classes.

Recyclability Studies

The main advantage of using a heterogeneous catalyst as an iron source for Fenton oxidation is its ease of removal from the treated water and reusability. The synthesized IOGOC was subjected to subsequent Fenton oxidation employing the same conditions at each run. Table 4 shows that there is a decrease in the efficiency after the first cycle but there was no significant difference in the removal for the succeeding cycles. This indicates that the synthesized IOGOC can be used repeatedly with little to no decrease in dye removal efficiency after the first cycle. However, it can also be observed that there is a general decrease in the adsorption capacity of the reused composite, which can be attributed to the incomplete removal of adsorbate on the surface of the adsorbent.

Table 4. Recyclability of synthesized IOGOC composite.

Run number	% dye removed[a]	Adsorption capacity, mg CBB/g IOGOC[a]
1	79.48 ± 7.01	19.27 ± 4.06
2	70.89 ± 3.82	8.61 ± 1.46
3	71.93 ± 1.82	4.95 ± 1.08
4	70.68 ± 1.00	8.26 ± 0.88

Conditions: [CBB] = 20 mg/L, m_{IOGOC} = 10 mg, [PS] = 5 mM, pH = 3.0, T = 25 °C, adsorption time = 90 min, contact time = 240 min, shaking velocity = 200 rpm.; [a]Expressed as mean SD (n = 3)

CONCLUSION

An IOGOC is synthesized and utilized as an adsorbent and as an activator of the persulfate oxidant that facilitated the degradation and removal of CBB R-250 in aqueous solutions. Characterization of the synthesized composite indicates the presence of GO and Fe_3O_4, which is most likely magnetite in the nanoscale. Adsorption isotherm modeling on the CBB R-250 adsorption on IOGOC reveals that it follows the Langmuir isotherm model with a maximum adsorption capacity of 14.31 mg CBB R-250/g IOGOC, indicating a formation of a monolayer of adsorbate on the surface of the adsorbent. The adsorption process follows the pseudo-second-order kinetic model.

An acidic pH for the starting solution is desired since this is a good environment for the release of iron ions from the composite structure, favoring the activation of persulfate in the mixture. Based on the working dye concentration range, the highest removal percentage is obtained at 10 mg/L CBB solution. Higher adsorbent dosages, as well as higher persulfate concentrations, result in a higher amount of CBB removed from the mixture due to the presence of more oxidant and catalyst for the generation of radicals that will trigger the dye degradation process.

End product analyses reveal that the use of IOGOC provides a lower amount of dissolved iron in the resulting solution, which is within the limits set by the Water Quality Guidelines and General Effluent Standards of 2016. COD experiments, on the other hand, indicate that there is a 73% removal of COD but the amount of organic material is still higher than what is recommended. Recyclability studies show that IOGOC can be used repeatedly without a significant decrease in dye removal efficiency.

ACKNOWLEDGMENTS

The authors appreciate the contributions and assistance of Dr. Florinia E. Merca and Dr. Lilia M. Fernando of the National Institute of Molecular Biology and Biotechnology at the University of the Philippines Los Baños during the conduct of the study.

REFERENCES

ALRUMMAN A, EL-KOTT F, ATTALLA S. 2016. Water Pollution: Source & Treatment. American Journal of Environmental Engineering 6(3): 88–98.

ANDREWS G. 2018. Resolving the Water Pollution Crisis in the Philippines: The Implications of Water Pollution on Public Health and the Economy. Pepperdine Policy Review, Vol. 10, Article 2.

ATA S, IMRAN DIN M, RASOOL A, QASIM I, UL MOHSIN I. 2012. Equilibrium, thermodynamics, and kinetic sorption studies for the removal of Coomassie Brilliant Blue on wheat bran as a low-cost adsorbent. Journal of Analytical Methods in Chemistry 1(1): 1–8.

BABURAJ MS, ARAVINDAKUMAR CT, SREEDHANYA S, THOMAS AP, ARAVIND UK. 2012. Treatment of model textile effluents with PAA/CHI

and PAA/PEI composite membranes. Desalination 288: 72–79.

BARIK R, JENA BK, DASH A, MOHAPATRA M. 2014. *In situ* synthesis of flowery-shaped α-FeOOH/Fe_2O_3 nanoparticles and their phase dependent supercapacitive behaviour. RSC Adv 4(36): 18827–18834.

BRADDER P, LING SK, WANG S, LIU S. 2011. Dye adsorption on layered graphite oxide. Journal of Chemical and Engineering Data 56(1): 138–141.

CHEN X, XUE Z, YAO Y, WANG W, ZHU F, HONG C. 2012. Oxidation degradation of rhodamine B in aqueous by UV/$S_2O_8^{2-}$ treatment system. International Journal of Photoenergy 2012: 1–5.

CLARKE EA, ANLIKER R. 1980. Organic dyes and pigments. In: Handbook of environmental chemistry; Part A: anthropogenic compounds. Hutzinger O ed. New York: Springer. p. 181–215.

[DENR] Department of Environment and Natural Resources. 2016. Water Quality Guidelines and General Effluent Standards of 2016 [DAO 2016-08]. Retrieved from http://pab.emb.gov.ph/wp-content/uploads/2017/07/DAO-2016-08-WQG-and-GES.pdf

EATON AD, CLESCERI LS, GREENBERG, AE, FRANSON MAH, [APHA] American Public Health Association, [AWWA] American Water Works Association, [WEF] Water Environment Federation. 1998. Method 3500-Fe B and 5220; D. Standard methods for the examination of water and wastewater. Washington, DC: APHA.

FOO KY, HAMEED BH. 2010. Insights into the modeling of adsorption isotherm systems. Chemical Engineering Journal 156(1): 2–10.

FURMAN OS, TEEL AL, WATTS RJ. 2010. Mechanism of base activation of persulfate. Environ Sci Technol 44(16): 6423–6428.

GOVINDAN K, RAJA M, MAHESHWARI SU, NOEL M. 2015. Analysis and understanding of amido black 10B dye degradation in aqueous solution by electrocoagulation with the conventional oxidants peroxomonosulfate, peroxodisulfate and hydrogen peroxide. Environmental Science: Water Research and Technology 1(1): 108–119.

GUPTA H, KUMAR R, PARK HS, JEON BH. 2016. Photocatalytic efficiency of iron oxide nanoparticles for the degradation of priority pollutant anthracene. Geosystem Engineering 20(1): 21–27.

HERRERA F, LOPEZ A, MASCOLO G, ALBERS P, KIWI J. 2001. Catalytic combustion of Orange II on hematite surface species responsible for the dye degradation. Applied Catalysis B: Environmental 29(2): 147–162.

JOHRA RT, LEE J-W, JUNG W-G. 2014. Facile and safe graphene preparation on solution based platform. Journal of Industrial and Engineering Chemistry 20(5): 2883–2887.

KHAN MA, ALAM MM, NAUSHAD M, ALOTHMAN ZA, KUMAR M, AHAMAD T. 2015. Sol-gel assisted synthesis of porous nano-crystalline Co-Fe_2O_4 composite and its application in the removal of brilliant blue-R from aqueous phase: an ecofriendly and economical approach. Chemical Engineering Journal 279: 416–424.

KONICKI W, ALEKSANDRZAK M, MIJOWSKA E. 2017. Equilibrium, kinetic and thermodynamic studies on adsorption of cationic dyes from aqueous solutions using graphene oxide. Chemical Engineering Research and Design 123: 35–49.

LI G, DENG R, PENG G, YANG C, HE Q, LU Y, SHI H. 2018. Magnetic solid-phase extraction for the analysis of bisphenol A, naproxen and triclosan in wastewater samples. Water Science and Technology 77(9): 2220–2227.

LI X, ZHENG X, TANG K. 2015. Study of adsorption properties of anionic dyes on graphene oxide/chitosan composite porous microspheres. XXXIII IULTCS Congress, (Chakraborty 2003), p. 1–8.

LI YS, CHURCH JS, WOODHEAD AL. 2012. Infrared and Raman spectroscopic studies on iron oxide magnetic nano-particles and their surface modifications. Journal of Magnetism and Magnetic Materials 324(8): 1543–1550.

MAHANTA D, MADRAS G, RADHAKRISHNAN S, PATIL S. 2008. Adsorption of sulfonated dyes by polyaniline emeraldine salt and its kinetics. Journal of Physical Chemistry B 112(33): 10153–10157.

MARCANO DC, KOSYNKIN DV, BERLIN JM, SINITSKII A, SUN Z, SLESAREV A, ALEMANY LB, LU W, TOUR JM. 2010. Improved Synthesis of Graphene Oxide. ACS Nano 4(8): 4806–4814.

MURA S, JIANG Y, VASSALINI I, GIANONCELLI A, ALESSANDRI I, GRANOZZI G, CALVILLO L, SENES N, ENZO S, INNOCENZI P, MALFATTI L. 2018. Graphene Oxide/Iron Oxide Nanocomposites for Water Remediation. ACS Appl Nano Mater.

NAMDURI H, NASRAZADANI S. 2008. Quantitative analysis of iron oxides using Fourier transform infrared spectrophotometry. Corrosion Science 50(9): 2493–2497.

NIDHEESH PV, GANDHIMATHI R, RAMESH ST. 2013. Degradation of dyes from aqueous solution by Fenton processes: a review. Environmental Science and Pollution Research 20(4): 2099–2132.

OUYANG ZW, CHEN EC, WU TM. 2015. Thermal Stability and Magnetic Properties of Polyvinylidene Fluoride/Magnetite Nanocomposites. Materials 8(7): 4553–4564.

PAZ A, CARBALLO J, PÉREZ MJ, DOMÍNGUEZ JM. 2017. Biological treatment of model dyes and textile wastewaters. Chemosphere 181: 168–177.

PÉREZ-GUZMÁN MA, ORTEGA-AMAYA R, SANTOYO-SALAZAR J, ORTEGA-LÓPEZ M. 2020. Urea-based synthesis of magnetite nanoparticles and its composite with graphene oxide: structural and magnetic characterization. Journal of Material Science: Materials and Electronics 31: 7490–7498.

RAMESHA GK, VIJAYA KUMARA A, MURALIDHARA HB, SAMPATH S. 2011. Graphene and graphene oxide as effective adsorbents toward anionic and cationic dyes. Journal of Colloid and Interface Science 361(1): 270–277.

RASOULIFARD MH, ABBASIOUN N, GHALAMCHI L. 2018. Enhanced oxidation of azo dye using Ag-SiO_2 nanoparticle and peroxydisulfate and kinetic study. Journal of Sciences, Islamic Republic of Iran 29(1): 27–34.

ROBINSON T, MCMULLAN G, MARCHANT R, NIGAM P. 2001. Remediation of dyes in textile effluent: a critical review on current treatment technologies with a proposed alternative. Biores Technol 77: 247–255.

SALES PF, MAGRIOTIS ZM, ROSSI MALS, RESENDE RF, NUNES CA. 2013. Optimization by Response Surface Methodology of the adsorption of Coomassie Blue dye on natural and acid-treated clays. Journal of Environmental Management 130: 417–428.

SAXENA S, TYSON TA, SHUKLA S, NEGUSSE Z, CHEN H. 2011. Investigation of structural and electronic properties of graphene oxide. Appl Phys Lett 99: 013104.

SUN Q, YANG L. 2003. The adsorption of basic dyes from aqueous solution on modified peat-resin particle. Water Res 37: 1535–1544.

TAN KL, HAMEED BH. 2017. Insight into the adsorption kinetics models for the removal of contaminants from aqueous solutions. Journal of the Taiwan Institute of Chemical Engineers 74: 25–48.

WENG CH, TAO H. 2015. Highly efficient persulfate oxidation process activated with Fe^0 aggregate for decolorization of reactive azo dye Remazol Golden Yellow. Arabian Journal of Chemistry 11(8): 1292–1300.

[WWAP] United Nations World Water Assessment Programme. 2017. The United Nations World Water Development Report 2017. Wastewater: The Untapped Resource. UNESCO, Paris.

YANG X, ZHANG X, MA Y, HUANG Y, WANG Y, CHEN Y. 2009. Superparamagnetic graphene oxide-Fe_3O_4 nanoparticles hybrid for controlled targeted drug carriers. J Mater Chem 19: 2710–2714.

YAO Y, MIAO S, YU S, PING MA L, SUN H, WANG S. 2012. Fabrication of Fe_3O_4/SiO_2 core/shell nanoparticles attached to graphene oxide and its use as an adsorbent. Journal of Colloid and Interface Science 379(1): 20–26.

ZHANG J, AZAM S, SHI C, HUANG J, YAN B, LIU Q, ZENG H. 2015. Poly(acrylic acid) Functionalizes Magnetic Graphene Oxide Nanocomposite for Removal of Methylene Blue. RSC Advances. DOI: 10.1039/C5RA01815C